Printed Conductive Transparent Films for the Fabrication of Sensors by Aerosol Inkjet Systems

Marissa E. Morales Rodriguez[1, 2], Peter L. Fuhr[1]

[1]Oak Ridge National Laboratory, One Bethel Valley Road, Oak Ridge, Tennessee, 37831 USA
[2]The Bredesen Center for Interdisciplinary Research and Graduate Education at the University of Tennessee, 418 Greve Hall, 821 Volunteer Blvd., Knoxville, Tennessee, 37996, USA

Abstract – *Fabrication of sensors using additive manufacturing printers holds the promise for low-cost sensors for continuous and real time monitoring of physical and chemical parameters in industrial settings. Aerosol inkjet systems have demonstrated the capability to print small feature sizes with high precision using a variety of materials. Advances in nanomaterials suitable for use by such printers raises the possibility of having transparent, conductive films and sensors. Typically, transparent conductive films are fabricated using metallic oxides and complicated procedures on rigid substrates. In this paper, we present the results of the combination of silver nanowires formulations and aerosol inkjet systems for the fabrication of transparent conductive films by printing and its characterization. Implications for utilization of conductive, transparent sensors in manufacturing and industrial processes settings are discussed.*

Key Words: Transparent conductive films, printed electronics, aerosol inkjet, sensors, silver nanowires

1. INTRODUCTION

Printed electronics combines the field of advanced materials, additive manufacturing (AM) and electronics, Figure 1. Formulations of nanoparticles or nanomaterials have made possible the further development of the printed electronic (PE) "field". PE provides the possibility for rapid printing of complicated patterns using single or combination of materials and holds promise for possible mass fabrication of electronics on rigid and flexible substrates. There is a wide array of AM technologies and associated printers that may be used for sensor fabrication. Advancements in printing technologies have led to the rapid development of printed sensors, radio frequency identification tags (RFID) batteries, light emitting diodes (LED), and solar cells, just to mention a few [1-14].

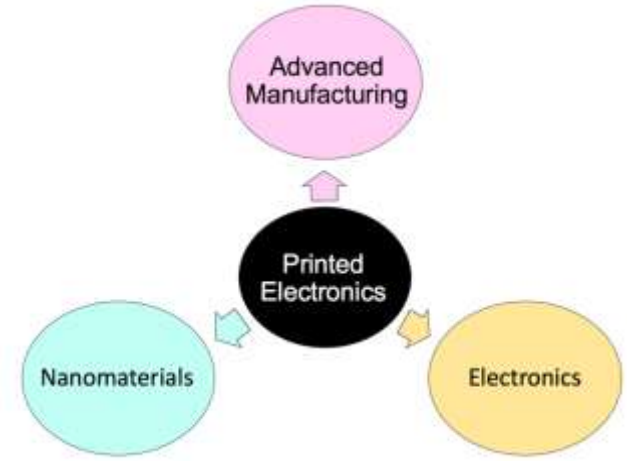

Fig 1: Printed electronics is the combination of three fields

Printed electronics is a technology that originated in the 1950s with gravure printing. The evolution of additive manufacturing systems, incorporating nanomaterials have propelled the invention of new printers for electronics. Printed electronics offers rapid prototyping, simple process, low fabrication cost and high volume production [15-17]. Printed electronics systems can be divides in two groups, non-contact and contact printing. The printing method is selected depending on the application, feature resolution, substrate (flexible or rigid), ink and temperature of the process. In this context, an ink refers to the nanomaterials used to print conductive patterns. As previously mentioned, there are multiple systems to develop electronics by printing. Screen printing, inkjet printing and aerosol jet printing, and laser induced forward transfer (LIFT) are non-contact techniques. This means that the ink deposition head is never in contact with the substrate. This feature is very useful when printing on 3D substrate is desired. Screen printing is commonly used for large scale manufacturing and mass production of devices like RFID tags and antennas, just to mention some examples. During the inkjet printing, a drop on demand approach that uses piezoelectric transducer at the nozzle head to deposit the ink on the substrate [18].

This work was conducted at Oak Ridge National Laboratory, managed by UT-Battelle LLC for the US Department of Energy (DOE) under contract DE- AC05-00OR22725.

Rigid and flexible substrates are compatible with this technique [19]. The distance between the nozzle and the substrate is about 1 – 2 mm and droplet size are about 16 µm in diameter. Inkjet printing shares some similarities with aerosol jet printing. Both techniques are compatible with a broad range of materials and offer small feature sizes for non-contact techniques. In the aerosol jet printing technique, a sheath gas ejects the ink out of the nozzle as a focused beam depositing feature sizes around 10 µm on a substrate. Rigid, flexible and 3D substrates can be used with this system. The distance between the nozzle and the substrate is about 3 – 5 mm and the aerosol droplets size are about 1 – 5 µm in diameter. The aerosol jet printer is the latest technology in printed electronics. It offers two modes of ink deposition, pneumatic atomizer and ultrasonic atomizer. Depending on the ink viscosity and nanoparticle size one chooses one deposition method versus the other.

The aerosol jet system is able to print the smallest feature to date, for a non-contact technique, and provides the flexibility to print on any substrate using any ink. It also offers the possibility to be scaled up for mass production. A typical direct printing procedure consists of three steps. First, designing a pattern using a software drafting application like AutoCAD. The design is loaded to the printer, where the operating software convert it to a tool path with a series of commands for printing the desired pattern. The second step is to start deposition of the ink to print the pattern on the substrate, followed by temperature post processing of the deposited film. Temperature post processing of the film consist of heating the substrate with the printing design to evaporate the solvent and anneal the film to form a continuous, smooth conductive thin film [20]. Sheet resistance is a metric for the characterization of conductive thin films and can be defined as;

$$R = \frac{\rho}{t}\frac{L}{W} = R_s\frac{L}{W} \quad (1)$$

where, L is the film length, W is the width and R_s is the sheet resistance with units of ohms per square (Ω/square) [21].

The curing and annealing temperatures and time depend on the nanoparticle formulations and the desired substrate. For example, flexible substrates must be cured at room temperatures (up to 300 °C) whereas rigid substrates can tolerate higher temperatures. In the printed electronics process, the curing post printing process is critical for the performance of the printed film. The curing and annealing temperatures and time depend on the nanoparticle formulations and the desired substrate. For example, flexible substrates must be cured at room temperatures (up to 300 °C) whereas rigid substrates can tolerate higher temperatures.

There are many types of printing techniques and technologies that may be used in fabricating electronic circuits. While lithographic processes are, by far, the most prevalent and most used in high density semiconductor circuit and system fabrication, there are other technologies that are viable for the manufacture of certain types of electronics. The printing processes presented in this Section focused on the three techniques that are the most promising in providing low cost, (relatively) rapid printing of electronic circuits using conductive inks.

1.1 Conductive Nanomaterials for Printed Electronics

Nanomaterials are integral components for the development and evolution of the printed electronics field. Conductive materials are used for direct wiring of different patterns. Figure 2, summarizes the electrical conductivity of different materials. Although, the most commonly used materials are metals, printed electronics have opened the door for direct writing of patterns using organic materials like PEDOT/PSS and other materials like graphene, carbon nanotubes. Ceramics like indium titanium oxide (ITO), are used as conductive materials but due to the high temperature process is it not used in printed electronics.

The conductive materials used as inks to write patterns on different substrates are typically nanoparticle based solutions. There are different methods for the nanoparticles synthesis in the literature [22-28]. Most of the synthesis routes include a polyol process from a $AgNO_3/Cl^-/PVP/EG$ solution [29].

Formulations with different mass loading (w/w%) and particle size range of about 5-500 nm are used as long as it meets the viscosity requirements of the printer. In addition, the pH of the formulation is typically neutral to avoid corrosion of the printer's nozzles and deposition mechanism.

Electrical conductivity comparison of wiring materials for PE

Materials		Electrical conductivity (Siemens/cm)	Notes
Metals	Ag	6.2×10^5	Bulk properties
	Cu	5.9×10^5	
	Au	4.4×10^5	
	Pt	1.0×10^5	
	Ni	1.4×10^5	
Organic	PEDOT/PSS	$1–10^3$	
Ceramics	ITO	$10^3–10^4$	Depends on doping/composition, oxygen defects, and crystallinity High-temperature treatment required
	CNT	1×10^5 cm²/V s ($\sim10^4$ S/cm for CNT fiber [1])	Theoretical values of single-wall (SW) CNT electron mobility (electron mobility of Si is approx. 10^3 cm²/V s). Depends on carrier concentration
	Graphene	2×10^5 cm²/V s	One- and two-dimensional materials

Fig 2: Printed electronics is the combination of three fields

1.2 Nanomaterials for Printed Transparent Conductive Films

Printed electronics, specifically roll-to-roll fabrication, have made possible the development and possible large scale manufacturing of transparent electronics. This activity seems concentrated on optically transparent coatings and covers for displays, photovoltaics and similar products – not sensors – using fabrication techniques and facilities costing in the 10's to 100's of millions of dollars.

Transparent conductive films (TCF) have multiple applications in today's electronics. Typically, a material defined as TCF exhibits 70% transmittance in the visible spectrum and sheet resistance of less than 10^3 ohms per square [30]. Electronic devices with TCF components include liquid crystal displays, touch screens, plasma displays, organic light emitting diodes. One of the most commonly used materials used are doped metallic oxides, such as indium tin oxide (ITO). There are a number of complications when using metallic oxides, for example, complicated and time consuming processes that include vacuum conditions. In addition, after processing they require high temperature processes (400C) to achieve low sheet resistance which make them unsuitable to use with temperature sensitive substrates. In addition, they are brittle in nature limiting their application in flexible electronics. In the past decades, efforts have been made to develop new materials for TCF. These materials include, conductive polymers, carbon nanotubes, graphene, and metallic nanowires. Alternatives materials to ITO films can be used as inks for direct printing at room temperature and films annealing at lower temperatures for fabrication of TCFs on brittle and flexible substrates.

Table 1 provides a summary of the materials used to fabricate TCFs and the performance of the film. The summary focuses on the materials that can be used as inks formulations for PE printers. Several studies have reported the used of organic PEDOT/PSS and carbon nanotubes (CNTs) in combination with inkjet printers for the fabrication of TCFs. Both materials can be found commercially available or by customizing the formulations.

This study focuses on the fabrication of TCFs and sensors using the combination of silver nanowires and aerosol jet printer. To this date, there has been no report on using this particular combination of nanomaterial and printer. Based on the aerosol jet printer's characteristics and the conductivity and transparency characteristics, metallic nanowires are chosen as the appropriate material for this research. Although metallic nanowires can be made out different metals, silver is commonly used. Therefore, the examination focuses on silver metallic nanowires. As described above, fabrication of TCFs can be possible at room temperatures suitable for printing techniques. With a reminder that there are different printing techniques that can be employed for printing sensors - including inkjet printing, screen printing and aerosol jet - these methods exhibit different features and require different specification of the inks selected[30]. One of the challenges, therefore, is to find a metallic nanowire ink compatible with the non-contact aerosol jet printer. For the aerosol jet system, for example, an ink compatible with the printer is required to meet the specifications for optimization of the ink deposition and to avoid clogs in the deposition head nozzle tip.

Table 1: Summary of nanomaterials for TCF fabrication

Material	Sheet Resistance Ω/sq	Transparency %	Layer Thickness	Curing Temperature °C	Deposition Method	Substrate
ITO[31]	30	80	240 nm	500	Sputtering, spin or drop coating by sol gel	Glass
Graphene[32]	30	90	~2 nm	N/A	CVD	Copper
Graphene-AgNWs (Hybrid)[33-35]	>30	90	Not reported	Not reported	CVD/drop coating	Flexible Polymer
MCNTs[19,36]	1.1×10^6	>95	300 nm	Not reported	Inkjet	Preheated Glass
MWCNTs-PEDOT/PSS[36]	3.5×10^3	~98	300 nm	Not reported	Inkjet printing	Preheated Glass
SWCNTs-PEDOT/PSS[37]	150	80	300 nm	80	Inkjet printing	Flexible Polymer
PEDOT/PSS[38]	200-600	Not reported	600 nm	25-60	Inkjet printing	Glass and flexile polymer
Metallic Nanowires (silver)[23, 26, 27, 39][23]	8	50	0.5-2 µm	110	Inkjet printing	Flexible polymer
	5-9	90	Not reported	200	Drop coating and roll-to-roll	Glass and Flexible polymer

2. MATERIALS AND METHODS

As mentioned in the introduction section, the fabrication by printing of TCFs and sensors on this study will focus on the utilization of silver nanowires formulations as inks for the aerosol jet system. Three different AgNWs formulations were used as inks with the aerosol jet system Two customized formulations of short length AgNWs were developed upon which the printing procedures of transparent conductive films for transparent sensors was based. The formulation of 2.7-micron length fibers with diameter of 39 nm and a concentration of 3.80 wt% silver (3170), <25wt% polyvinylpyrrolidone in isopropyl alcohol (IPA) was supplied by Nanogap. A second formulation, from Nanogap, of AgNWs of 3.4 µm length and 45nm in diameter with nanowires suspended in IPA with a mass loading of 2.85wt% silver was also used. The last set of experiments were conducted using a AgNWs formulation commercially available purchased from Sigma Aldrich. This formulation commercially available contain silver wires of 60 nm diameter and 10 µm length, 0.5wt% silver in IPA suspension lot #MKCC8584 (739421). The compatibility of the longer length AgNWs and the atomization process is a determined factor for the success of the fabrication of the transparent films and sensors using an aerosol jet system. Let's consider that during the aerosol atomization process, the atomizer breaks the ink into small droplets of size of 1-5 µm. In addition, the recommended particle size is up to 500 nm.

The solutions were shaken well by hand prior to use because sonication can damage the fibers. Approximately 2mL of this solution were placed in the ink vial of the ultrasonic atomizer for printing.

As it is standard in printed electronics systems, a file with the desired designed was created to print features. An aerosol jet printer (AJ200) from, OPTOMEC, was used in this work. This system is capable of printing any ink on virtually any substrate with feature sizes as small as 10 µm.

2.1 Printing Parameters for Different AgNWs Formulations

The printing parameters associated with each AgNWs formulations are described in Table 2. For each formulation a parameter associated with the atomization process of the ink is found. During the atomization process, the sheath gas pushes' the ink out of the deposition head nozzle as a focused aerosol jet. Therefore, optimum parameters are needed for the optimum atomization of the AgNWs formulations. A full description of the atomization process of the aerosol jet system can be found elsewhere [40].

Table 2: Description of printing parameters of the aerosol inkjet system

AgNWs length (µm)	2.7	3.4	10
Printed Feature Size	~20 µm	~20 µm	~20 µm
Deposition Head Tip	100 µm	150 µm	150 µm
Platform Temperature	70 °C	70 °C	70 °C
MFC Sheath	35 sccm/ 2.3 psi	45 sccm/ 1.21 psi	50 sccm/ 1.6 psi
MFC UA Atomization	20 sccm/ 3.75 psi	50 sccm/ 3.32 psi	50 sccm/ 2.8 psi
UA current	0.3 mA	0.39 mA	0.42 mA
Process Speed	2 mm/sec	1-1.5 mm/sec	2 mm/sec
Curing Process 30 mins	300 °C	300 °C	300 °C
Total Print Time	~40 mins	~40 mins	~40 mins

3. RESULTS & DISCUSSION

TCF films were printed on a glass substrate using different parameters on the aerosol jet system. A 1 x 1 cm^2 square was designed using AutoCAD then converted into a print file which was loaded into the aerosol jet system. As the aerosol ink jet is deposited to the surface, the AgNWs form lines with the appearance of a mesh where electrons can flow between the intersecting points of the mesh. This specific network, or mesh, structure is what gives the AgNWs the conductivity characteristics. To fill the squares, lines of 20 µm thickness where overlapped by 0, 20, 50 and 80%. The same procedure was repeated for each AgNWs formulation. A visible representation of the resulting printed films is shown in Figure 3, which shows photographs of the AgNWs printed on the glass slide. For comparison, the glass slide was placed on a white and black background. When the glass slide is against the white background the films are invisible to the eye. On the contrary, when the glass slide is against the black background, the films appear to the eye as a hazy spot on the surface. As expected, the printed films using the 10 µm length AgNWs exhibit less transparency.

Transparency measurements were performed using an ultraviolet/visible spectrophotometer, model USB4000 from Ocean Optics. To perform these measurements, the samples were illuminated by an incandescent lamp with a multimode optical fiber placed behind the sample to collect the transmitted light from the sample and transport it to the spectrophotometer's detector. Spectra was collected for all the samples presented in Figure 3. Transparency measurements were collected for the glass background for comparison. The plots show the intensity counts versus the wavelengths emitted by the lamp. The printed TCFs showed excellent transparency compared to the background glass with values of over 97% transparency for the AgNWs with 2.7 and 3.4 µm in length. The compatibility of the longer length AgNWs and the atomization process is a determined factor for the success of the fabrication of the transparent films and sensors. It is worthwhile to reexamine the aerosol atomization process, where the atomizer breaks the ink into small droplets of size of 1-5 µm. In addition, the recommended particle size is up to 500 nm. To this date, the utilization of 10 µm length AgNWs as an ink for the aerosol jet system has not been reported. As expected, the transparency of the films is decreasing as the overlap of the lines is increasing. The optical characterization of these samples confirms this observation. The results of the transmittance of the sample in the UV/Vis region is shown in Figure 4. The light intensity as a function of wavelength was measured and the results shows the transparency of the samples decrease significantly by increasing the line overlap which translate to an increase in mass loading on the glass substrate. The samples showed a decrease in transparency of approximately 74%, 60%, and ~1% of the light.

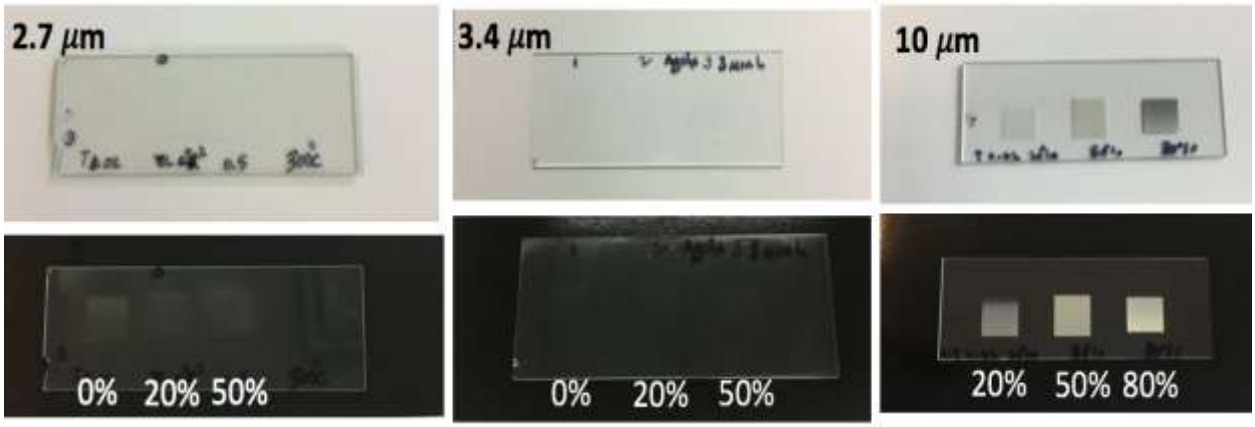

Fig 3: Pictures of the printed TCFs on glass slide. Films where printed using different formulations of AgNWs with different lengths. Three films where printed with 20, 50, and 80% overlap of the printed lines

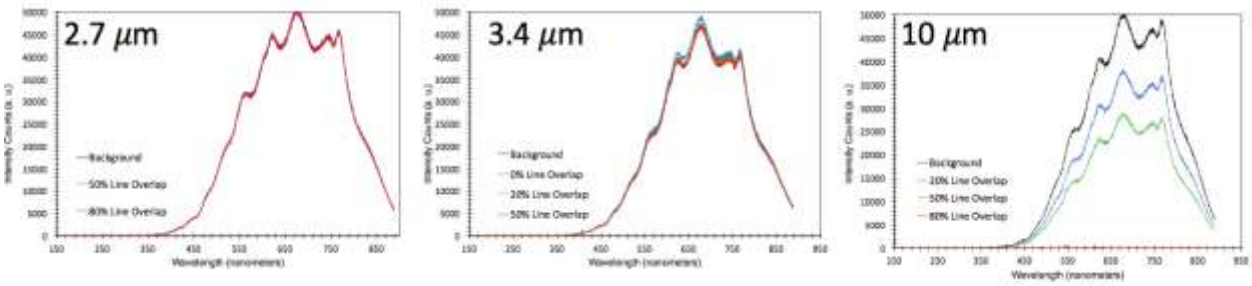

Fig 4: Spectral characterization of the different TCFs

Optical microscopy characterization was performed to observe the topology of the films on the glass slide. The 50X micrographs are shown in Figure 5 for the TCFs printed overlapping the 20 μm lines by 50%. A random distribution of particles across the surface is observable. In addition, smaller particles, and agglomerates are observed across the surfaces making a network in some areas but shorted in others as in the case of the films printed with the 2.7 μm length AgNWs. The 3.4 μm length AgNWs formulation are approximately 0.7 μm longer, however, the mass loading is 1% less silver compared to the previous formulation used for this test. It is visible that a lower concentration of silver has a direct impact on the topology and particle concentration of the printed film. For this 3.4 μm length AgNWs sample, the micrograph shows small particles across the surface. It is clear that a wire network across the surface does not exist. This could be due to the combination of low mass loading of the solution and low density of the solution that can make the fibers airborne during the atomization process. This will reduce the amount of AgNWs deposited on the surface. In contrast to the shorter length wires, the 10 μm AgNWs form the expected mesh or network when deposited on a surface from solution. This network of connected wires gives a high probability of exhibiting conductivity of the resultant printed film.

The formulation with AgNWs of 10 μm in length yielded the expected topology for the fabrication of TCFs. Therefore, Figure 6 presents, the micrographs of the printed films overlapping the printed lines by 20, 50, and 80%. These micrographs were taken to monitor the mass loading changes as a function of the overlapping of the printed lines. There is a linear relationship with the overlapping of the lines increases and the mass loading. The film printed overlapping the lines by 80% exhibits a continuous structure with agglomerates across the surface.

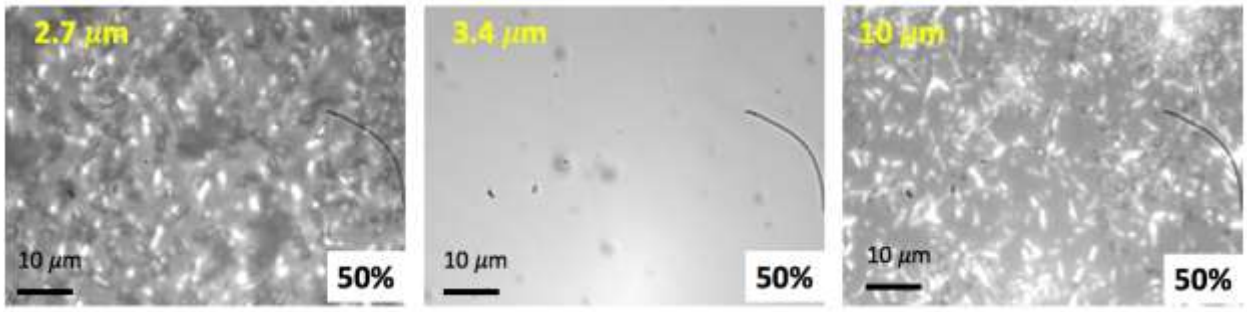

Fig 5: Micrograph (50X) comparison of printed films using AgNWs of 2.7, 3.4 and 10 μm in length overlapping the lines by 50%

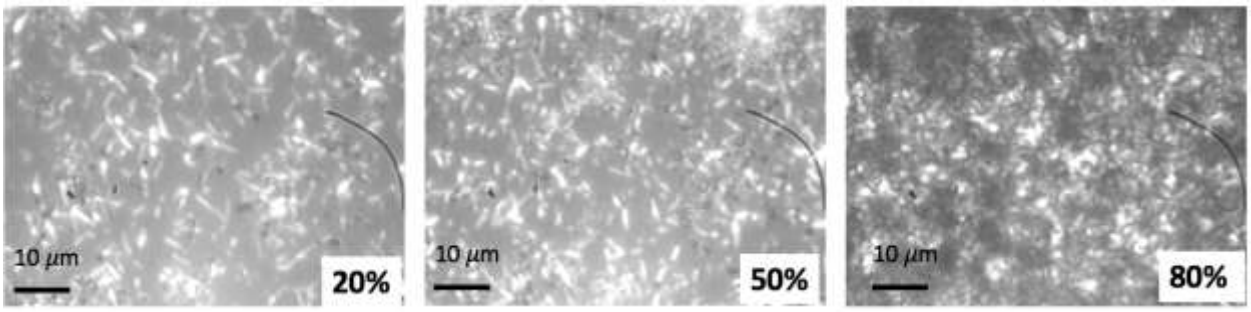

Fig 6: Micrograph (50X) of 10 μm AgNWs printed film on glass overlapping the printed lines by 20%, 50% and 80%

The sheet resistance of the printed films was measured using a four-point probe model RM3000 test unit from Jandel. The sheet resistance range of the RM3000 is from 1 milliohm-per-square up to 5 x 10^8 ohms-per-square with 0.3% accuracy, according to the manufacturer[1]. The cylindrical head used has probes of tungsten carbide with 200 μm radius and 0.635 mm spacing. The resistivity test performed revealed no conductivity for the samples printed with the 2. 7 μm AgNWs. The four-point probe made contact with the sample in four different areas of the 1 x 1 cm^2 sample. While performing the RM3000 Test Unit measurements, the unit's display showed "Contact Limit" indicating that the test unit was reporting a problem driving the current. This could be the result of the sample being too insulating as the current needles are not making proper contact with the sample.

The lack of conductivity in these samples can be attributed to different factors. For example, it was discussed that shape of the AgNWs could be losing their integrity during the atomization process, resulting in shorter wires or small particles with randomized shape. This can affect the expected formation of a network of wires, similar to a mesh, that allows the electrons to flow across the surface. Another consideration to keep in mind is that the needles of the cylindrical probe used to measure the sheet resistivity have radius of 200 μm compared to the ~2.7, 3.4 and 10 μm of the AgNWs. This means that the cross section of the needles and the fiber is very small to perform a measurable resistivity. The electrical test unit was set to 10 and 50mA applied current, for all the samples. The samples printed with 20% and 50% overlap of the lines displayed "contact limit" which means no measurable resistivity. However, the sample printed with 80% overlap of the lines showed sheet resistivity of ~0.159 Ω/□when 10mA was applied. The sheet resistivity for this film is an order of magnitude higher compared to 1 x 10^{-2} Ω/□for a film printed under the same conditions using a silver nanoparticle colloidal solution. The colloidal solution is Clariant EXPT PRELECT TPS G2 with particle size range of about 10-100 nm and silver content of 50 w% of silver, <20 w% ethenediol and water. The same study reported that the roughness of the film plays an important role on the conductivity of the sample [41].

High resolution images of the topography of the surface were taken by atomic force spectroscopy. Figure 6 shows topographic images, side by side, of the printed films with AgNWs of 2.7 μm in length and silver nanoparticle solutions. As has been mentioned throughout this discussion, once the thickness of the printed line is set, the aerosol jet printer fills the structures with multiple lines in a rastering fashion. The AFM images show the difference between the two printed films. In the case of the conductive film printed with the silver nanoparticle solution, the multiple printed lines, to fill the structure, are observed across the surface.

Figure 7 shows that the film printed with the AgNWs solution does not exhibit the same line structured features. The results of this characterization show that the surface of the AgNWs printed films combines, large particles agglomerations and small features. The large particle agglomerations form surface steps of about 150 nm height, according to the surface profile. The surface profile shows spikes at the top of the large agglomerations features on the surface with heights range from 15-90 nm. The topology also shows small features across the surface with length of less than 2 μm. Considering that the AgNWs used are about 2.7 μm length, breakage of the AgNWs could have occurred during the atomization process. During this process the solution is placed on an ultrasonic water bath that breaks the solution into droplets to form the aerosol. This could have contributed to poor conductivity properties of the printed films.

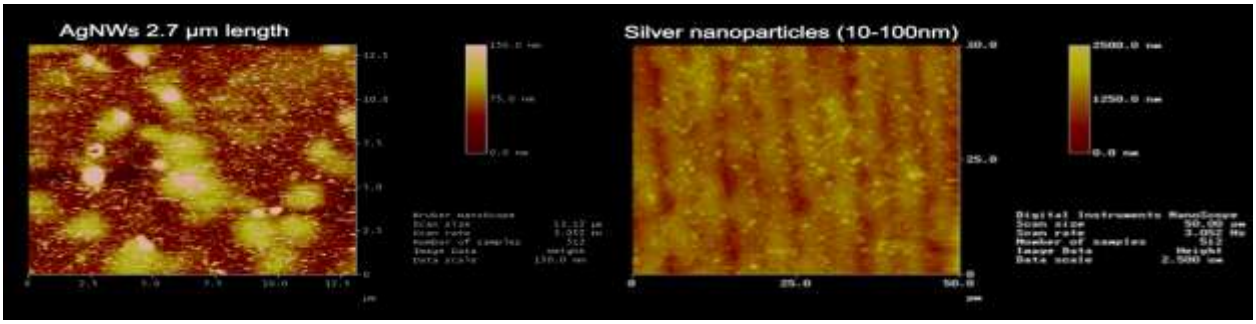

Fig 7: AFM topographic images for comparison of printed films with AgNWs and silver nanoparticles solutions

[1] Bride Technology Four Point Probe Jandel RM3000 Test Unit. Four-point-probes.com/rm3000-test-unit-with-pc-software/ (Accessed May 2017)

4. CONCLUSIONS

The fabrication of transparent films via an aerosol jet printer using conductive AgNWs inks has been demonstrated with applications to transparent sensors. A procedure to fabricate conductive, transparent films and sensors using such the combination of aerosol inkjet system and silver nanowires formulations has been developed and discussed. This worked showed that formulations with silver nanowires larger than 500nm in particle size can be atomized and deposited using the aerosol jet system. Particle sizes up to 500 nm is recommended to use with this particular system. This work opens the door for the optimization of nanowires formulations for the fabrication of transparent systems using this printing technology.

Transparent films and sensors are crucial in a wide variety of industrial and manufacturing situations. We have demonstrated that an aerosol jet printer may be used for cost-effective rapid prototyping and associated small, medium, large-scale fabrication of sensors. The flexibility of printing films and sensors leads to providing a means for cost-effective measure of critical material behavior and guide a process to achieve desired properties would greatly enhance the process productivity and yield. For industrial and manufacturing settings, this is often the most important, yet most elusive, process improvement.

The technical details and challenges associated with this class of printed electronics, aerosol jet printing – using the appropriate inks – are discussed. Further optimization is needed on the formulation of inks for transparent conductive films and sensors compatible with the aerosol jet inkjet system. Such optimization consists on the focusing of the ink jet and optimum mass loading for transparency and conductivity properties.

ACKNOWLEDGMENTS

This manuscript has been authored by UT-Battelle, LLC under Contract No. DE-AC05-00OR22725 with the U.S. Department of Energy. The United States Government retains and the publisher, by accepting the article for publication, acknowledges that the United States Government retains a non-exclusive, paid up, irrevocable, worldwide license to publish or reproduce the published form of this manuscript, or allow others to do so, for United States Government purposes. The Department of Energy will provide public access to these results of federally sponsored research in accordance with the DOE Public Access Plan (http://energy.gov/downloads/doe-public-access-plan).

REFERENCES

1. Khan, S.; Dang, W.; Lorenzelli, L.; Dahiya, R. Flexible Pressure Sensors Based on Scre en-Printed P(VDF-TrFE) and P(VDF-TrFE)/MWCNTs. IEEE Transactions on Semiconductor Manufacturing, **2015,** 28 (4).
2. Khan, S.; Tinku, S.; Lorenzelli, L.; Dahiya, R.S. Flexible tactile sensors using screen printed P(VDF-TrFE) and MWCNT/PDMS composites. IEEE Sensors Journal **2015,** 15 (6), 3146.
3. Khan, S.; Lorenzelli L.; and Dahiya, R.S. Bendable piezore- sistive sensors by screen printing MWCNT/PDMS composites on flexible substrates. In 10th Conference on Pd.D. Research in Microelectronics and Electronics (PRIME), 2014; pp 1-4.
4. Khan, S.; Doh, Y. H.; Khanb, A.; Rahman, A.; Choi, K.H.; and Kim, D. S. Direct patterning and electrospray deposition through EHD for fab- rication of printed thin film transistors. Current Applied Physics **2011,** 11
5. Kim, T.; Jung, Y. H., Chung, H.; Yu, K.J.; Ahmed, N.; Corcoran, C.J.; Park, J.; Jin, S.H.; and Rogers, J.A. Deterministic assembly of releasable single crystal silicon-metal oxide field-effect devices formed from bulk wafers. Applied Physics Letters **2013,** 102.
6. Sandström, A.; Dam, H.F.; Krebs, F.C.; and Edman, L. Ambient fabrication of flexible and large-area organic light-emitting devices using slot-die coating. Nature Communications **2012,** 3 (Art ID 1002).
7. Zheng, Y.; He, Z.; Gao, Y.; Liu, J. Direct Desktop Printed-Circuits-on-Paper Flexible Electronic. Scientific Reports **2013,** 3
8. Jung, M.; Kim, J.; Noh, J.; Lim, N.; Lim, C.; Lee, G.; Kim, J.; Kang, H.; Jung, K.; Leonard, A.D; Tour, J.M; Cho, G. All-Printed and Roll-to-Roll-Printable 13.56-MHz-Operated 1-bit RF Tag on Plastic Foils. IEEE Transactions on Electron Devices **2010,** 57 (3).
9. Kang, H. W.;Sung, H.J.;, Lee, T.; Kim, D.; Kim, C. Liquid transfer between two separating plates for micro-gravure-offset printing. Journal of Micromechanics and Microengineering **2009,** 19 (1)
10. Deganello, D.; Cherry, J.A.; Gethin, D.T.; Claypole, T.C. Patterning of micro-scale conductive networks using reel-to-reel flexographic printing. Thin Solid Films **2010,** 518 (21).
11. Khan, S.; Lorenzelli, L.; Dahiya, R. S. Technologies for Printing Sensors and Electronics Over Large Flexible Substrates: A Review. IEEE Sensors Journal **2015,** 15 (6), 3164
12. Kaufmanna,T.; Ravoo, B.J. Stamps, inks and substrates: polymers in microcontact printing. Polymer Chemistry **2010,** 1.
13. Radha, B.; Lim, S. H; Saifullah, M.; Kulkarni, G. U. Metal hierarchical patterning by direct nanoimprint lithography. Scientific Reports **2013,** 3.

14. Chang, W.; Fang, T.; Lin, H.; Shen, Y.; Lin, Y. A Large Area Flexible Array Sensors Using Screen Printing Technology. Journal of Display Technology **2009,** 5 (6).

15. Nathan, A.; Ahnood. A.; Cole, M.; Lee, S.; Suzuki. Y.; Hiralal, P.; Bonaccorso, F.; Hasan, T.; Garcia-Gancedo, L.; Dyadyusha, A.; Haque, S.; Andrew, P.' Hofmann, S.; Moultrie, J.; Chu, D.; Flewitt, A.J.; Ferrari, A.C.; Kelly, M.; Robertson, J.; Amaratunga, G.; Milne, W. Flexible electronics: The next ubiquitous platform. Proceedings of IEEE **2012,** 100, 1486-1517.

16. R. Fabian Pease; Chou, S. Y. Lithography and Other Patterning Techniques for Future Electronics. Proceedings of IEEE **2008,** 96 (2).

17. Søndergaard, R.; Hosel, M.; Krebs, F. Roll-toRoll fabrication of large area functional organic materials. Journal of Polymer Science Part B Polymer Physics **2012,** 51 (1), 16.

18. Helmholtz Association of German Research Centres. Inkjet printing process for kesterite solar cells. (accessed February).

19. Kim, B.; Geier, M.L.; Hersam, M.C.; Dodabalapur, A. Inkjet Printed Circuits on Flexible and Rigid Substrates Based on Ambipolar Carbon Nanotubes with High Operational Stability. Applied Materials and Interfaces **2015,** 7 (50).

20. Greer, J.R.; Street, R.A. Thermal cure effects on electrical performance of nanoparticles silver inks. Acta Materialia **2007,** 55.

21. Ellingson, R.; Heben, M. Sheet Resistance: Measurement and Significance. http://astro1.panet.utoledo.edu/~relling2/teach/archives?4580.6280.2011/20111025_lecture_4.2_phys4580.6280.pdf (accessed January).

22. Wakuda, D.; Hatamura, M.; Suganuma, K. Novel method for room temperature sintering of Ag nanoparticle paste in air. Chemical Physics Letters **2007,** 441 (4).

23. Sun, Y. Silver nanowires - unique templates for synthesis of functional nanostructure. Nanoscale **2010,** 2 (9).

24. Wiley, B.; Sun, Y.; Mayers, B.; Xia, Y. Shape-controlled synthesis of metal nanostructures: the case of silver. Chemistry - A European Journal **2005,** 11 (2).

25. Wanga, H.; Qiao, X.; Chen, J.; Wang, X.; Ding, S. Mechanisms of PVP in the preparation of silver nanoparticles. Materials Chemistry and Physics **2005,** 94 (2-3), 449.

26. Sun, Y.; Gates, B.; Mayers, B.; Xia, Y. Crystalline Silver Nanowires by Soft Solution Processing. Nano Letters **2002,** 2 (2).

27. Abbasi, N.M.; Yu, H.; Wang, L.; Abdin, Z.; Amer, W.; Akran, M.; Khalid, H.; Chen, Y.; Saleem, M.; Sun, R.; Shan, J. Preparation of silver nanowires and their application in conducting polymer nanocomposites. Materials Chemistry and Physics **2015,** 166 (15).

28. Jiu, J.;Murai, K.; , Kim, Kim, D.; Kim, K.; Suganuma, K. Preparation of Ag nanorods with high yield by polyol. Materials Chemistry and Physics **2009,** 114 (2).

29. Tang, X.; Tsuji, M. Synthesis of Silver Nanowires in Liquid Phase. In Nanowires Science and Technology, Lupu, N., Ed. INTECH, 2010.

30. Suganuma, K., Introduction to Printed Electronics. SpringerBriefs in Electrical and Computer Engineering: 2014.

31. Chen, Z.; Li, W.; Li, R.; Zhang, Y.; Xu, G.; Cheng, H. Fabrication of highly transparent and conductive Indium-Tin Oxide thin films with a high figure of merit via solution processing. Langmuir **2013,** 29, 13836.

32. Bae, S.; Kim, S.j.; Shin, D.; Ahn, J. H.; Hong, B.H. Towards industrial applications of graphene electrodes. Physica Scripta **2012,** T146 (014024).

33. Lee, M.; Kim, J.; Park, J.; Park, J. U. Studies on the mechanical stretchability of transparent conductive film based on graphene-metal nanowire structures. Nanoscale Research Letters **2015,** 10 (27), 1.

34. Lee, M.; Lee, K.; Kim, S.; Lee, H.; Park, J.; Choi, K.; Kim, H.; Kim, D.; Lee, D.; Nam, S.; Park, J. High-Performance, transparent, and stretchable electrodes using graphene–metal nanowire hybrid structures. Nano Letters **2013** 13 (6), 2814.

35. Park, J.; Kim, J.; Kim, K.; Kim, S. Cheong, W.; Park, K.; Song, J.; Namgoong, G.; Kim, J.J.; Heo, J.; Bien, F.; Park, J.U. Wearable, wireless gas sensors using highly stretchable and transparent structures of nanowires and graphene. Nanoscale **2016,** 8

36. Zhou, W.; Belay, A. B.; Davis, K.; Sorloaica-Hickman, N. Transparent conductive film fabrication by carbon nanotube ink spray coating and ink-jet printing. In Photovoltaic Specialists Conference, IEEE: Austin, TX, USA, 2012.

37. Shimoni, A.; Azoubel, S.; Magdassi, S. Inkjet printing of flexible high-performance carbon nanotube transparent conductive films by "coffee ring effect". Nanoscale **2014,** 6, 11084.

38. Perinka, N., Kim, C.H.; Kaplanova, M.; Bonnassieux, Y. Preparation and characterization of thin conductive polymer films on the base of PEDOT:PSS by ink-jet printing. Physics Procedia **2013,** 44, 120.

39. Ye, T.; Jun, L.; Hu, W.; Ping, C.; Ya-Hui, D.; Zheng, C.; Yun-Fei, L.; Hao-Ran, W.; Yu, D. Inkjet-printed Ag grid combined with Ag nanowires to form a transparent hybrid electrode for organic electronics. Organic Electronics **2017,** 41, 179.

40. Vaezi, M.; Chianrabutra, S.; Mellor, B.; Yang, S. Multiple material additive manufacturing- Part 1: a review. Virtual and Physical Prototyping **2013,** 8 (1).

41. Morales-Rodriguez, M.E.; Joshi, P.; Humphries, J.; Fuhr, P.L.; McIntyre, T. Fabrication of low cost surface acoustic wave sensors using direct printing by aerosol jet. IEEE Access **2017**